

# Preparation of NiO Catalyst on FeCrAl Substrate Using Various Techniques at Higher Oxidation Process

Darwin Sebayang<sup>1</sup>, Yanuandri Putrasari<sup>1</sup>, Sulaiman Hasan<sup>1</sup>,  
Mohd Ashraf Othman<sup>1</sup> and Pudji Untoro<sup>2</sup>

<sup>1</sup>*Universiti Tun Hussein Onn Malaysia,*

<sup>2</sup>*Badan Tenaga Nuklir Nasional*

<sup>1</sup>*Malaysia*

<sup>2</sup>*Indonesia*

## 1. Introduction

Catalytic converter consists of three major components, i.e substrate, catalyst, and washcoat. The first one is a substrate, a support for catalyst material. The FeCrAl is generally considered as metallic substrates due to their advantage in the high-temperature corrosion resistance, including the strong adherence of oxide film on the surface of substrate when applied the appropriate surface treatment (Twigg & Webster, 2006; Pilone, 2009; Klower et al., 1998; Cueff et al., 2004; Badini & Laurella; 2001; Czyrska-Filemonowicz et al., 1999; Liu et al., 2001; Amano et al., 2008; Checmanowski & Szczygiel, 2008). This material is based on ferritic steels with 5-8 wt% aluminium, 17-22 wt% chromium, plus small additions of reactive elements, which are added to improve the oxidation resistance and oxide adhesion (Nicholls & Quadakkers, 2002). Meanwhile, a catalyst is the accelerate agent for chemical reaction in terms of oxidation and reduction of emission gas. The existing of excellent oxidation catalyst materials was usually based on the precious metal (Pt, Pd, and Rd). However, those materials are expensive and limited supply (Koltsakis & Stamatelos, 1997; Benson et al., 2000). For this reason, the cheaper ranges of oxides (e.g. CuO, V<sub>2</sub>O<sub>5</sub>, NiO, MoO<sub>3</sub>, and Cr<sub>2</sub>O<sub>3</sub>) compared to precious metals are being investigated as an alternative catalyst (Kolaczowski, 2006). This work reports the use of NiO catalyst developed from Ni as a starting material. A washcoat is a catalysts carrier with high surface area. This material is usually an oxide layer such as Al<sub>2</sub>O<sub>3</sub>, SiO<sub>2</sub>, TiO<sub>2</sub>, or SiO<sub>2</sub>-Al<sub>2</sub>O<sub>3</sub> (Heck et al., 2002). Nickel forms under a normal temperature and pressure conditions only one oxide, NiO. The mechanism by which oxidation of a nickel proceeds was involved the outward migration of cations and electrons, which forming a single-phase scale (Birks et al., 2006). The conventional technique for adhering catalyst on substrate is by washcoating techniques that generally comprise of preparing a coating formed from a high surface area oxide blended with one or more catalysts and dipping the monolith structure into that coating blend (Huang & Bar-Ilan, 2003; Eleta et al., 2009). One of the most common methods to form a thin layer of oxide coatings on the metallic substrate is dip coatings, which combined with some

pre-treatments, such as growing a number of textured alumina whiskers on the surface of the metal support and shortened the diffusion path before depositing the washcoat (Zao, et al., 2003; Jia et al., 2007). The other methods are co-precipitation, sol-gel and spray-pyrolysis methods were also applied for preparation of FeCrAlloy supported perovskite for catalytic combustion of methane (Yanqing, et al., 2010). Furthermore, another technological procedure to develop and adhere to the catalysts on the FeCrAl substrate are based on electrophoretic deposition (Sun et al., 2007; Corni et al., 2008), solution combustion synthesis (SCS) (Specchia et al., 2004), aluminizing technique (Wu et al., 2007), and hydrothermal method (Zamaro et al., 2008; Wei et al., 2005; Mies et al., 2007; Sivaiah, 2010). However, the existing methods still have some limitations, especially due to the rather complicated method to applying the catalyst which is in the form of powder. This paper presents an innovative method for preparation of NiO catalyst on FeCrAl substrate through the combination of electroplating, ultrasonic treatment and oxidation process. Electroplating method was applied to coat Ni to the FeCrAl. The ultrasonic treatment was used in order to accelerate the solid particles to high velocities (Suslick et al., 1999). And, the oxidation process was aimed to convert Ni into NiO on the FeCrAl surface and to develop Al<sub>2</sub>O<sub>3</sub> layer as well.

## 2. Methodology

### 2.1 Materials

The FeCrAl foils strip (Aluchrom YHf) was supplied by ThyssenKrupp VDM, Germany. The chemical compositions of the specimen according to ThyssenKrupp Data Sheet No. 4049 are listed in Table 1. The Al<sub>2</sub>O<sub>3</sub> powders, SiC powders, nickel sulphamate (Ni(SO<sub>3</sub>NH<sub>2</sub>)<sub>2</sub>·4H<sub>2</sub>O), nickel chloride (NiCl<sub>2</sub>·6H<sub>2</sub>O), boric acid (H<sub>2</sub>BO<sub>3</sub>), sodium lauryl sulphate (C<sub>12</sub>H<sub>25</sub>SO<sub>4</sub>Na), hydrochloric acid (HCl), sodium hydroxide (NaOH), methanol (99%), ethanol (99%) and nickel plates (high-purity Ni) were obtained from Sigma Aldrich, Sdn. Bhd. (Malaysia).

	Ni	Cr	Fe	C	Mn	Si	Al	Zr	Y	Hf	N
min	-	19.0	bal	-	-	-	5.5	-	-	-	-
max	0.3	22.0		0.05	0.50	0.50	6.5	0.07	0.10	0.10	0.01

Table 1. Chemical composition (wt. %) of FeCrAl

### 2.2 Experimental procedures

The approach started with assessment of FeCrAl treated by using various nickels electroplating process based on the weight gain during oxidation, followed by short term oxidation process, and long term oxidation process. The steps are summarized in flowchart as shown in Figure 1.

#### 2.2.1 First step: Assessment of FeCrAl treated using various nickel electroplating process

In this study, the various electroplating processes of nickel on the FeCrAl were carried out as the preliminary study to obtain the optimum method to develop nickel oxide on the FeCrAl substrate.

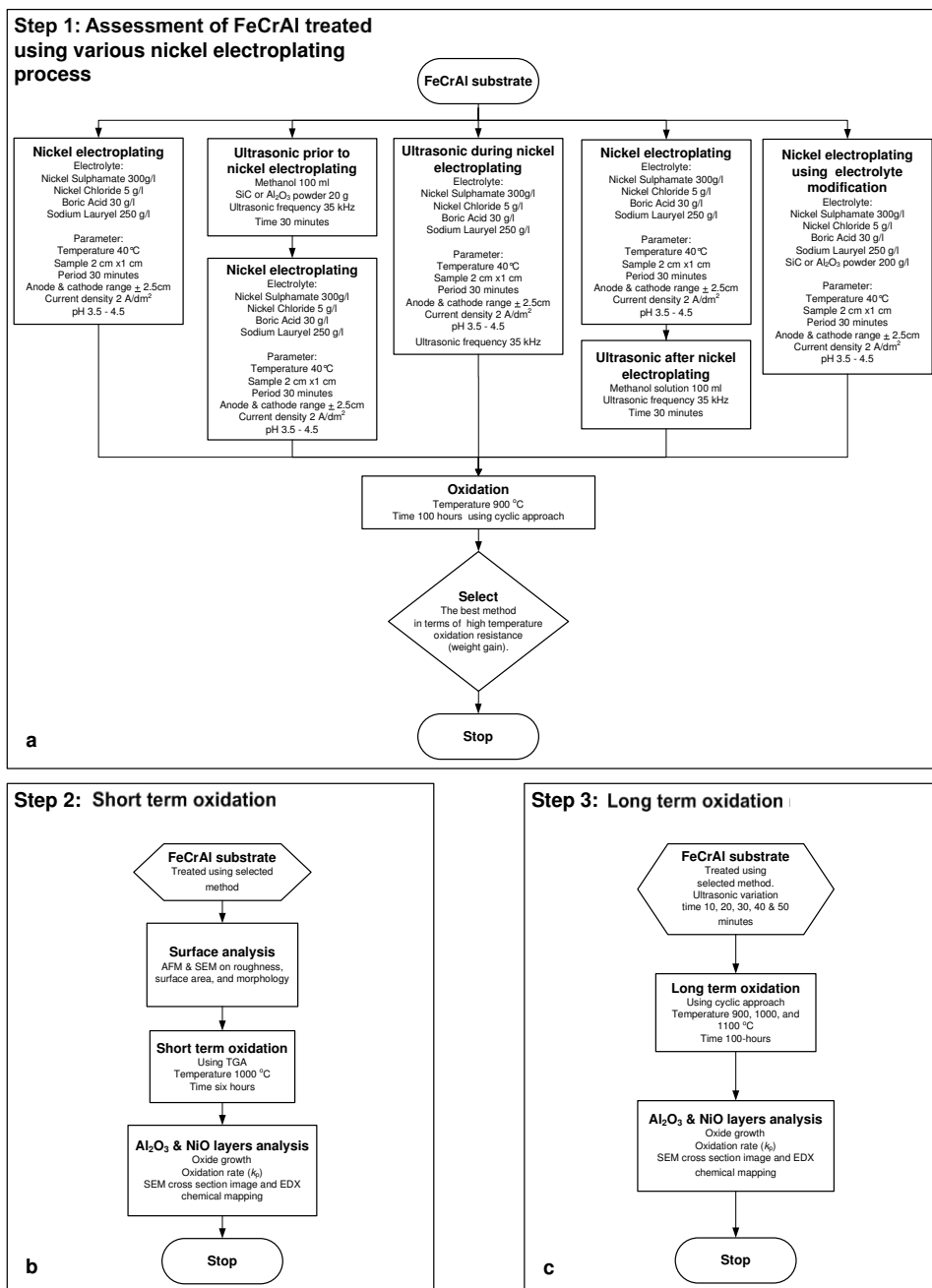


Fig. 1. Flow chart of the research, a) assessment of FeCrAl treated using various nickel electroplating, b) short term oxidation, c) long term oxidation

The study analyzed the influence of various electroplating processes of nickel on the FeCrAl metallic monolith for high-temperature oxidation resistance. The proposed new ideas to adhere to nickel as a catalyst on the FeCrAl substrate is divided into five methods as follows: Nickel electroplating, ultrasonic treatment prior to, during, and after nickel electroplating, and nickel electroplating using electrolyte modification. The optimum result in terms of high-temperature oxidation resistance which obtained from this investigation was then selected for further study/testing.

### 2.2.1.1 Nickel electroplating

The nickel electroplating process was conducted according to Rose & Whittington (2002). The following equipments, e.g. laboratory power supply, retorch clamp, hot plate magnetic steering, glass beaker, petri disc, and, etc. were used for electroplating process. The sample testing of FeCrAl foil was cut into 2 cm x 1 cm, and surface cleaned using ethanol. A solution was prepared by mixing 300 g/l of nickel sulphate powder and 5 g/l of nickel chloride powder, which dissolved into one litre of distilled water in a beaker glass. The concentration of 30 g/l of boric acid was then added to the solution, and pH value was maintained between 3.5 - 4.5. Boric acid acts as a buffer, to control the pH of the solution. The FeCrAl substrate was attached as a cathode and nickel plate (4 cm x 1 cm) as an anode. Both specimens then dipped simultaneously into the solution. The distance of the cathode-anode was set at the minimum 2.5 cm. The current density was setup at 2 A/dm<sup>2</sup>. During the experiment, bubbles occurred at the surface of the sample and the pH was fluctuated. To remove the bubbles, 0.1% of sodium lauryl sulphate (SLS) was added. H<sub>2</sub>SO<sub>4</sub> or NaOH solutions were added to maintain the pH. The electroplating process was started after 30 minutes. The specimen then dried. The condition of electroplating process is presented in Table 2, and the illustration of the electroplating process is shown in Figure 2.

Electroplating Condition	Parameter
Temperature of electroplating	40 °C
pH of electrolyte	3.5-4.5
Size of sample	2 cm x 1 cm
Electroplating period	30 minutes
Type of bath	Nickel sulphamate bath
Anode and cathode range	Min. 2.5 cm

Table 2. Electroplating process condition

### 2.2.1.2 Agitation using ultrasonic prior to, during, and after nickel electroplating

The *Fritsch Loborette 17* ultrasonic cleaning bath was used to conduct the ultrasonic process. The technical data in the ultrasonic apparatus were as follows: Voltage of 230 V/1~, input power of 2 x 240 W/period, frequency of 50-60 Hz and the ultrasound frequency of 35 kHz. Figure 3 (i) shows the condition for ultrasonic prior to electroplating process (pre-treatment). In this method, not only using methanol as a sonication media, Al<sub>2</sub>O<sub>3</sub> or SiC was also mixed with methanol 200 g/l. Meanwhile, the particle size distribution of Al<sub>2</sub>O<sub>3</sub> or SiC powders was analyzed using *Cilas 1180*. The sonication was conducted for 30 minutes. After completing the sonication, then it was transferred to electroplating beaker and electroplated with similar to the normal electroplating process. The sonication process of the sample was carried out by mixing the methanol with Al<sub>2</sub>O<sub>3</sub> or SiC, which called as pre-treatment.

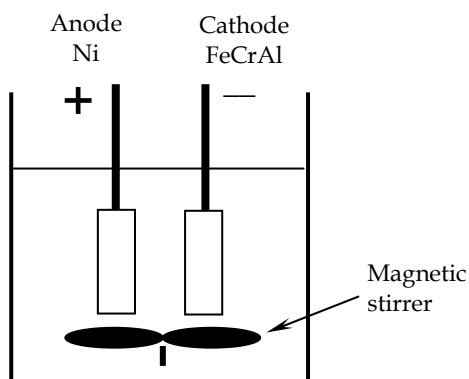


Fig. 2. Electroplating of FeCrAl alloy with nickel in a nickel sulphamate bath

Instead of just electroplating, ultrasonic process is also used to assist the nickel electroplating process. The condition of the electroplating process was similar with the previous, except the magnetic stirrer was replaced by ultrasound. The schematic diagram of the process is shown in Figure 3 (ii).

The ultrasonic process was also utilised after nickel electroplating process. In this method, the condition is similar to normal electroplating except the sonification was carried out after the electroplating process completed. The specimen was added into beaker glass with methanol solutions then sonicated for 30 minutes. The schematic diagram of the process is shown in Figure 3 (i).

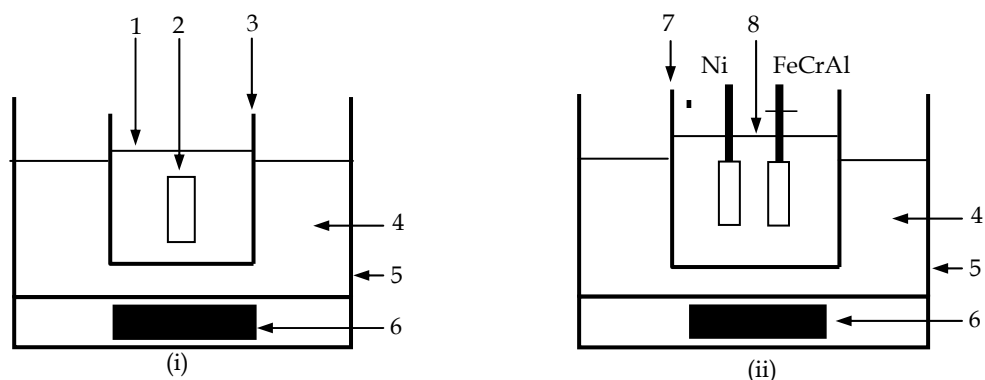


Fig. 3. (i) Schematic diagram of ultrasonic prior to (pre-treatment) and after electroplating process; (ii) Schematic diagram ultrasonic during electroplating process. (1) methanol; (2) specimen; (3) beaker; (4) water; (5) bath; (6) ultrasonic source; (7) plating tank; (8) electrolyte solution

### 2.2.1.3 Nickel electroplating using electrolyte modification

The new concept of electroplating was applied in this study to develop washcoat onto FeCrAl substrate, which done by mixing the electrolyte with 200 g/l of  $\text{Al}_2\text{O}_3$  or SiC powder. This method is similar to normal electroplating except the electrolyte was modified. During electroplating process, the electrolyte was agitated using a magnetic stirrer to dissolve  $\text{Al}_2\text{O}_3$  or SiC powder.

### 2.2.1.4 Oxidation process

The samples which produced by each variation method above were then oxidized to form the certain oxide ( $\text{Al}_2\text{O}_3$  or NiO). The uncoated FeCrAl substrate was also oxidized. The oxidation test in this study was conducted according to previous work by Badini & Laurella (2001) and ASTM G 54-84 (1996) standard. The *Carbolite* automatic high-temperature furnace model HTF 1800 was used for isothermal oxidation test with a cyclic approach (Nicholls & Quadackers, 2002; Fukuda, et al., 2002; Taniguchi, et al., 2002; Lylykangas & Tuomola, 2002). The test was carried out for 100 hours. The isothermal oxidation test with a cyclic approach is illustrated in Figure 4. The specimens were prepared by cutting them carefully into 5 mm x 5 mm. Then, the specimens were put in 5 mm diameter alumina crucible bucket. The weight of both specimen and bucket had been determined and recorded prior to oxidation test. The specimen that put in the alumina crucible bucket then delivered to the automatic furnace. The temperature was set-up of 30 to 910 °C of maximum temperature due to the catalytic converter working condition (Heck et al., 2002). The heating and cooling rate was set in 5 °C/minutes and holding time of 20 hours for each cycle. Then, the weight changes in every 20 hours were recorded. The testing was carried out until five cycle oxidation process. The weight of a specimen was measured, and the data was recorded after each cycle finished. The weight gains versus time graph were then plotted.

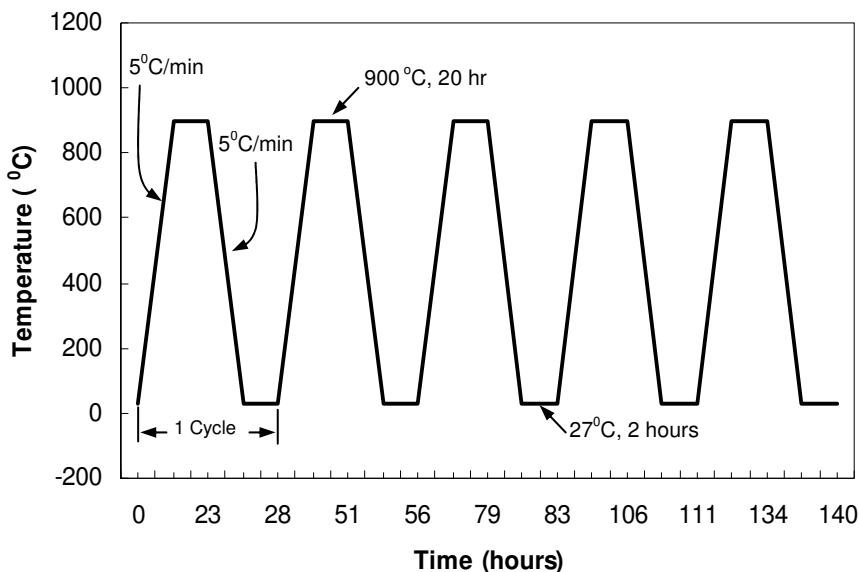


Fig. 4. Cyclic approach testing program (Adopted from Lylykangas & Tuomola, 2002)

### 2.2.2 Second step: Short term oxidation process

Prior to short term oxidation, the surface FeCrAl substrate was analysed in order to obtain the information of substrate surface, which previously treated using the selected method. The surface analysis was carried out by using step-and-scan automation of Atomic Force Microscopy (AFM) by *Park* model XE-100. Roughness (Ra) measurement was taken by horizontal straight-line mode. The Ra profiles were analysed and presented in order to clarify the roughness which caused by ultrasonic treatment of the FeCrAl surface specimens. The mean Ra is a result from a random 100  $\mu\text{m}^2$  scan area of specimens. The 3D images from AFM were presented to analyze the topography of a specimen. The grain area ( $\mu\text{m}^2$ ) as 2D image was measured by using AFM analysis to calculate the total surface area of a specimen. The scanned surface areas of a specimen were calculated and approached by spherical surface analysis (Henke et al., 2002). This approach was adopted for this research. The approach assumed that the grain morphologies as a nodule on FeCrAl substrate in half of sphere form. Then, the mean area obtained from AFM was assumed as an area of circles where the diameter similar to the sphere. The half of sphere surface area was calculated by using sphere surface area formula. The surface analyses were carried out after ultrasonic pre-treatment without nickel electroplating to observe any changes in surface characteristic. The short term oxidation analysis focused on weight gain, oxidation rate ( $k_p$ ), morphology of oxide layer and cross section elemental mapping of washcoat ( $\text{Al}_2\text{O}_3$  layer). Meanwhile, the oxidation test for six hours was conducted using *Diamond, Perkin Elmer* thermo gravimetric analyzer (TGA). The specimens were prepared by cutting into 2 mm x 2 mm. All of specimens are tested for oxidation by putting them into the TGA at 1000 °C for 360 minutes. Then, the data plotted into the graph of weight gain ( $\text{mg}/\text{mm}^2$ ) versus temperature (°C) or time (minutes). The graph was analyzed to obtain the parabolic rate constant (Smallman & Bishop, 1999; Badini & Laurella, 2001). The parabolic growth equation of the film thickness with time obtained by:

$$x^2 = k_p \cdot t \quad (1)$$

where  $x$  is the layer thickness or the weight gain;  $t$  is the oxidation treatment time;  $k_p$  is the parabolic rate constant. In this study, the weight gain ( $x$ ) is a resulted from mass gain per unit surface area of specimens  $\left(\frac{\Delta W}{A}\right)$  (Badini & Laurella, 2001). Then, the eq. (1) can be written as follow:

$$\left(\frac{\Delta W}{A}\right)^2 = k_p \cdot t \quad (2)$$

where  $k_p$  is obtained from the slope of a linear regression-fitted line of  $\left(\frac{\Delta W}{A}\right)^2$  vs  $t$  plot.

The microstructure analyses were carried out using JEOL Scanning Electron Microscope (SEM) model JSM-6380LA attached with Energy Dispersive X-ray (EDX). Prior to microstructure analysis, the specimen is mounted, ground and polished and coated with gold or platinum. The sample mounting conducted by hot press and cold mounting technique at a cross-sectional side of the specimen. The *Buehler* automatic hot mounting press machine was implemented for hot mounting process. The mounting parameters were 15 minutes mounting period, 2000 psi mounting pressure and 150 °C as the mounting temperature. For the cold mounting process, the ratio composition of resin and hardener

was 10 : 1. Then, the specimens were put into a mould at room temperature for minimum 24 hours until hardened. The specimens were ground using the SiC paper from 240 to 2000 grit, followed by polishing process, in order to obtain clear and shiny surface specimens.

After polishing, the specimens were observed under the digital microscope to ensure that the specimen did not have any scratches before further analyzed by SEM/EDX. The specimen was then coated with gold or platinum by using the sputter coating apparatus. The sputter coating was set in 20 mA of coating current and 20 minutes of coating time.

The back scattered mode of SEM was used to obtain a high-quality image of the specimen. The ranges of magnification, 100 x, 500 x, 1000 x, 1500 x and 2000 x, were used to observe both surface and cross-section of the specimen. The EDX mapping and line analysis techniques were also implemented in order to reveal the distribution of oxide layers on the FeCrAl surface substrate.

### 2.2.3 Third step: Long term oxidation process

This step is aimed to explore the behaviour of nickel layer on FeCrAl when subjected to the selected treatment at variation time for 10, 20, 30, 40 and 50 minutes, with high oxidation temperature for 100 hours. The oxidation process conducted using a cyclic approach testing, similar with previous sub section 2.2.1.4. To assess the high-temperature oxidation resistance of FeCrAl, the temperature oxidation of 1000 and 1100 °C were also applied. As similar with short term oxidation, in this step the oxide growth, and oxidation rate ( $k_p$ ) were also analysed. Nickel and nickel oxide morphologies were studied on the samples cross section at various temperatures. EDX attached to SEM was also used to obtain the elemental distribution of the samples cross section similar with sub section 2.2.2.

## 3. Results and discussion

### 3.1 Assessment of FeCrAl treated using various nickel electroplating process based on weight gain

The results of the isothermal oxidation at 900 °C in the air by cyclic oxidation test approach using an automatic high-temperature furnace presented in the graph of weight gain versus time as shown in Figure 5. The high weight gain of the FeCrAl due to poor high-temperature resistance. With more oxides developed during the elevated temperature, it will cause the substrate thickness of FeCrAl to decrease due to the transformation of its component to oxide. From this experiment, it can be seen that the electroplating of nickel will be a good barrier for the high-temperature resistance if treated with ultrasonic as well. The adhesions of nickel deposition on FeCrAl surface was improved by using the ultrasonic process. In this case, the ultrasonic process cause the collapse of cavitations bubbles of liquid and generates a pressure shock wave, liquid jet, and water hammer pressure. The ultrasonic act as an agitator, make faster stirring process. Thus, the electrolyte will mix properly as it is needed to fulfil the requirement of electroplating process (Chiba et al., 2000). From the results as mentioned above, it can be concluded that the ultrasonic pre-treatment cause the oxide grow sufficiently on the FeCrAl substrate and expected to have the capability for high-temperature oxidation resistance. Therefore, this method is selected and applied for further study.



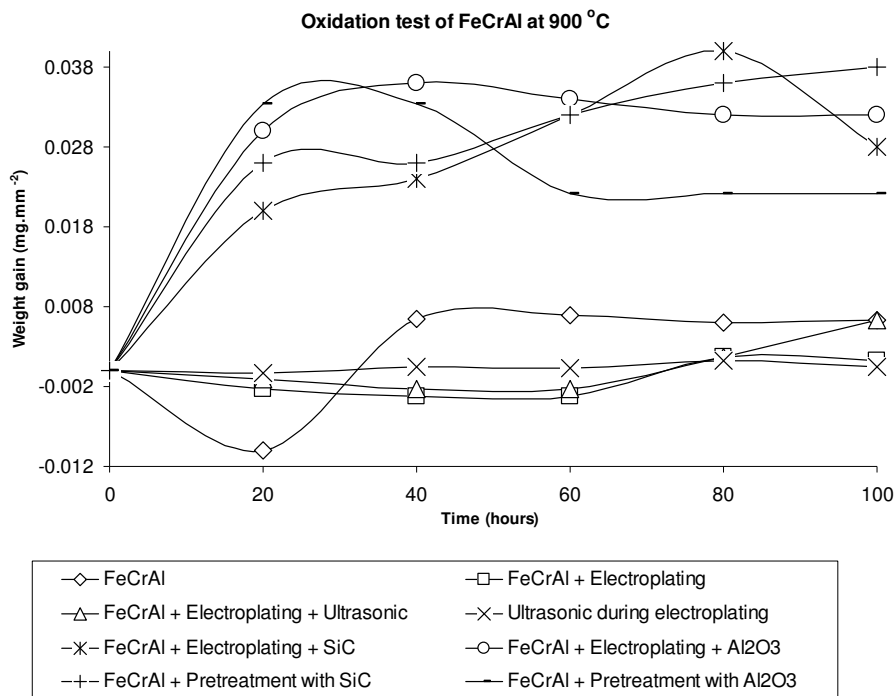


Fig. 5. Effect of various electroplating process on weight gain vs time of FeCrAl during oxidation at 900°C

### 3.2 Analysis of FeCrAl substrate before and after short term oxidation

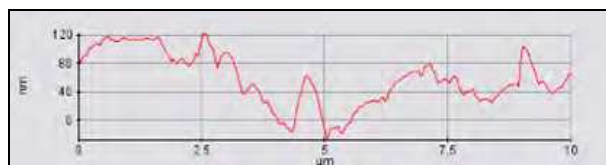
#### 3.2.1 Surface analysis

Figure 6 shows the roughness profile of the FeCrAl (a) untreated, (b) ultrasonic treatment with SiC for 10 minutes and (c) ultrasonic treatment with Al<sub>2</sub>O<sub>3</sub> for 10 minutes without nickel electroplating. From these profiles, the highest, medium, and lowest gap between peaks and valley occurred on FeCrAl untreated, treatment with Al<sub>2</sub>O<sub>3</sub> and with SiC, respectively.

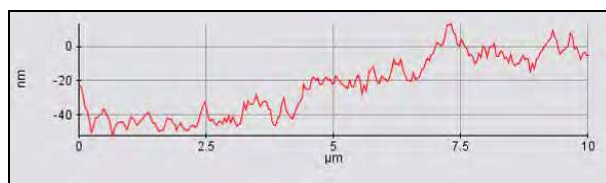
The mean roughness of FeCrAl was presented in Table 3. The mean roughness of each specimen was obtained by using the horizontal straight-line method on random position of 10 μm x 10 μm image. Meanwhile, the 3D images for all specimens were presented in Figure 7.

Materials	Mean Roughness, Ra (nm)
FeCrAl untreated	31.409
FeCrAl ultrasonic treatment with SiC	15.790
FeCrAl ultrasonic treatment with Al <sub>2</sub> O <sub>3</sub>	34.470

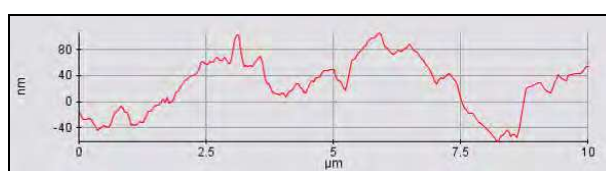
Table 3. Mean roughness of FeCrAl surface



(a)



(b)



(c)

Fig. 6. Roughness profile of FeCrAl surface a) untreated, b) ultrasonic treatment with SiC for 10 minutes, c) ultrasonic treatment with  $\text{Al}_2\text{O}_3$  for 10 minutes

Based on the roughness test results, the FeCrAl treated with  $\text{Al}_2\text{O}_3$  has the highest surface roughness value compared to the untreated and treated using ultrasonic with SiC. Based on the particle size distribution analysis that was conducted, for 60% distribution of  $\text{Al}_2\text{O}_3$  powder is  $42.07 \mu\text{m}$  with specific surface  $5658.19 \text{ cm}^2/\text{g}$  and 60% distribution of SiC powder is  $87.56 \mu\text{m}$  with specific surface only  $2279.44 \text{ cm}^2/\text{g}$ . It can be estimated that the roughness of FeCrAl surface depends on the particle size and homogeneity of the powders. The surface roughness of FeCrAl was as also estimated can be increased by the higher specific area of powders.

Figure 8 shows the grains of FeCrAl (a) untreated, (b) ultrasonic treatment with SiC for 10 minutes and (c) ultrasonic treatment  $\text{Al}_2\text{O}_3$  for 10 minutes. These images resulted from  $10 \mu\text{m} \times 10 \mu\text{m}$  random scanning area on each specimen. The grain numbers and grain area were presented in Table 4. The table shows that the grain numbers on FeCrAl ultrasonic treatment with SiC is the highest, followed by untreated FeCrAl, and the lowest is FeCrAl ultrasonic treatment with  $\text{Al}_2\text{O}_3$ . The highest grain area is FeCrAl ultrasonic treatment with  $\text{Al}_2\text{O}_3$ , then FeCrAl untreated, and the smallest is FeCrAl ultrasonic treatment with SiC.

Materials	Grain numbers	Mean area ( $\mu\text{m}^2$ )
FeCrAl untreated	172	$5.412 \times 10^{-1}$
FeCrAl ultrasonic treatment with SiC	183	$5.058 \times 10^{-1}$
FeCrAl ultrasonic treatment with $\text{Al}_2\text{O}_3$	167	$5.599 \times 10^{-1}$

Table 4. Mean of grain area on FeCrAl surface

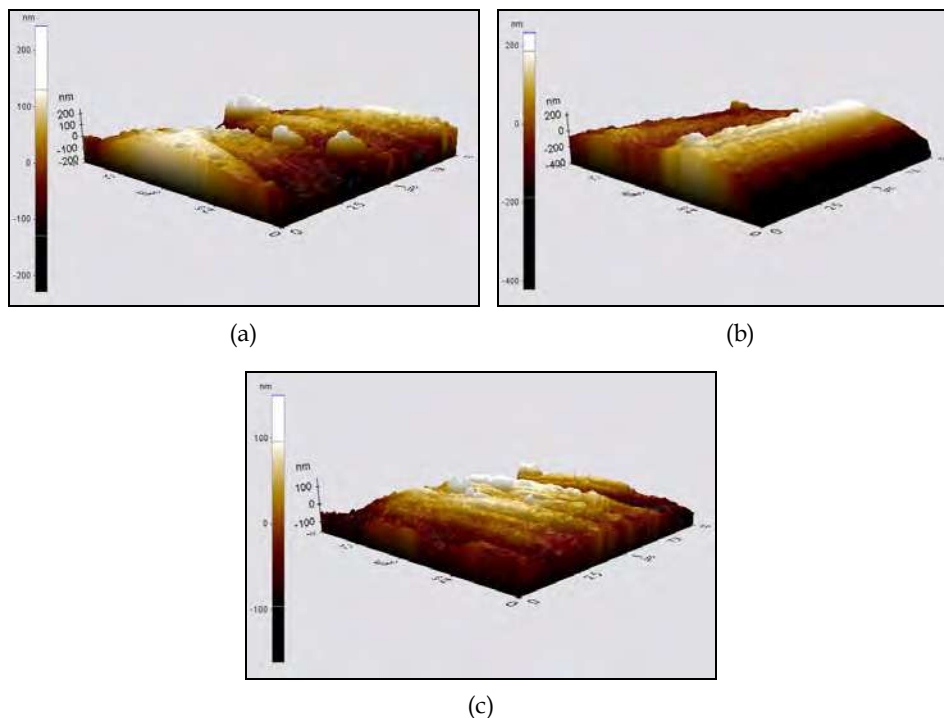


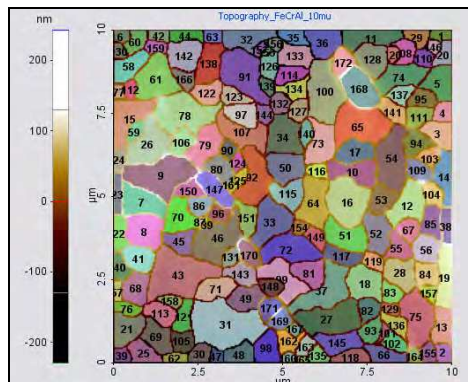
Fig. 7. Roughness 3D images of FeCrAl surface a) untreated, b) ultrasonic treatment with SiC for 10 minutes, c) ultrasonic treatment with Al<sub>2</sub>O<sub>3</sub> for 10 minutes

The surface area acts as a main role on the catalyst reaction effectiveness. In order to accommodate the catalyst in significant amounts, substrate must be provided with a high surface area. Twigg & Webster (2006) suggest that the design of substrate must provide a maximum superficial surface area which accommodates to the exhaust gas, as it is upon this surface that the catalytic coating is applied, and on which the pollutant and reactant gases must impinge in order to react.

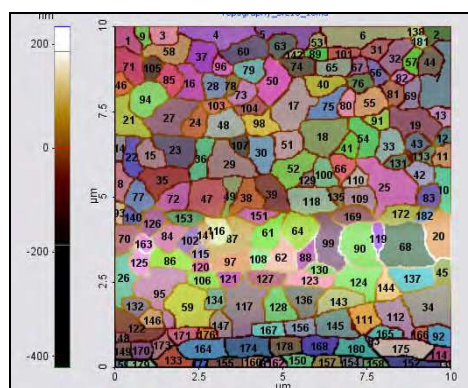
### 3.2.2 Parabolic rate constant

The parabolic rate constant ( $k_p$ ) can be used to predict the time to failure of the FeCrAl materials (Klower et al., 1998). The formation rate of an oxide scale, growing on the surface of a FeCrAl surface at the beginning of the oxidation test agrees with the Wagner theory. At high-temperature oxide, films are thickened according to the parabolic rate law,  $x^2 \propto t$  and the mechanism by which thickening proceeded has been explained by Wagner (Smallman & Bishop, 1999; Badini & Laurella, 2001).

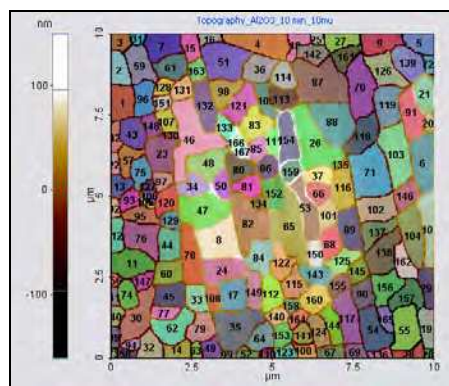
Figure 9 shows the nature of the fit of the parabolic rate law of the early oxidation test of FeCrAl substrate pre-treatment using ultrasonic with SiC or Al<sub>2</sub>O<sub>3</sub> at 1000 °C for 60 minutes. The parabolic rate constants obtained from the present experiments are listed Table 5. FeCrAl substrate pre-treated with SiC has lower  $k_p$  than the FeCrAl substrate pre-treated



(a)



(b)



(c)

Fig. 8. Grain area image of FeCrAl surface a) untreated, b) ultrasonic treatment with SiC for 10 minutes, c) ultrasonic treatment with  $\text{Al}_2\text{O}_3$  for 10 minutes

with  $Al_2O_3$ . The low of  $k_p$  value indicated the long time to failure of FeCrAl substrate (Klower et al., 1998). Thus, from these finding the FeCrAl substrate treated with SiC has better time to failure than treated with  $Al_2O_3$ .

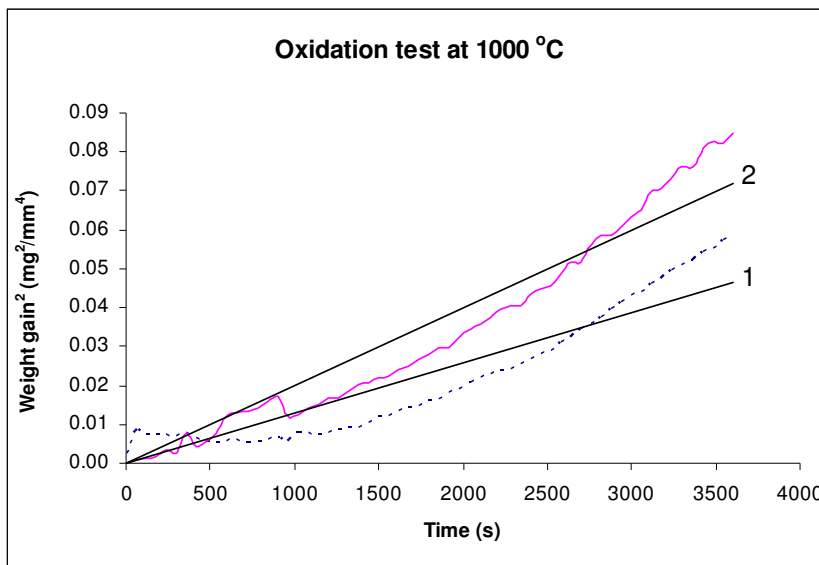


Fig. 9.  $\left(\frac{\Delta W}{A}\right)^2$  vs time plotted for oxidation of FeCrAl pre-treatment using ultrasonic prior to nickel electroplating with SiC (1) and with  $Al_2O_3$  (2)

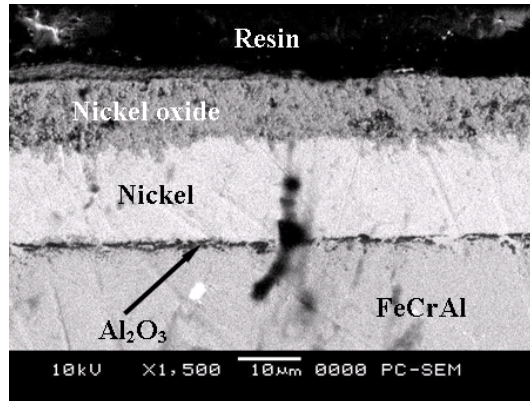
Materials	$k_p \times 10^{-6} \text{ mg}^2\text{mm}^{-4}\text{s}^{-1}$
FeCrAl substrate pre-treated with SiC	13
FeCrAl substrate pre-treated with $Al_2O_3$	20

Table 5. Parabolic rate constants for FeCrAl substrate pre-treated with SiC or  $Al_2O_3$  at 1000°C

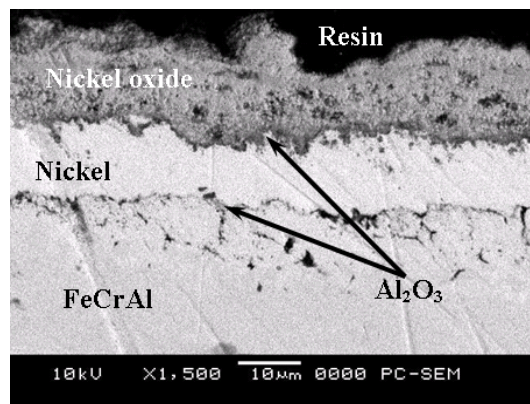
### 3.2.3 Cross section analysis of $Al_2O_3$ and NiO layers

Figure 10 shows the cross section scanning micrograph of the FeCrAl substrate pre-treatment using the ultrasonic process with SiC and  $Al_2O_3$  powder prior to nickel electroplating after short term oxidation. The cross-section of the images shows four layers. The first layer from bottom to top is FeCrAl substrate followed by  $Al_2O_3$  as the second layer, and the third is the nickel layer, and the fourth layer is the nickel oxide layer. The cross section observation showed that the NiO layer existed on the FeCrAl ultrasonic with SiC or  $Al_2O_3$  after short term oxidation.

Based on surface analysis, the ultrasonic process increased irregular surface roughness morphology on FeCrAl substrate. It might influence the homogeneous and stability of nickel electroplating, and also for NiO surface area development. The nickel electroplating on FeCrAl ultrasonic with SiC before electroplating showed more homogeneous, and it is a



(a)



(b)

Fig. 10. Cross-section scanning electron micrograph showing four layers of FeCrAl pre-treatment using ultrasonic with (a) SiC and (b)  $\text{Al}_2\text{O}_3$  prior to nickel electroplating after short term oxidation

more stable condition than  $\text{Al}_2\text{O}_3$ . Thus better density of nickel layer was achieved. Possibly, this was influenced by high surface roughness resulted from the FeCrAl substrate pre-treatment using ultrasonic with SiC. The cross section image clearly indicated that  $\text{Al}_2\text{O}_3$  and NiO layers occurred due to the heating process. However, the nickel layer still existed after short oxidation, so that needs further study.

### 3.3 Analysis of $\text{Al}_2\text{O}_3$ and NiO layers for long term oxidation

#### 3.3.1 Influence of various pre-treatment times and temperatures on weight gain and parabolic rate constant

The influence of various pre-treatment times on the weight gain of FeCrAl ultrasonic pre-treatment with SiC before electroplating and oxidized at 900, 1000, 1100 °C are shown in

Figure 11, 12, and 13, respectively. The influence of various pre-treatment times on the weight gain of FeCrAl ultrasonic pre-treatment with  $\text{Al}_2\text{O}_3$  before electroplating after oxidation at 900, 1000, and 1100 °C are presented also as a graph in Figure 14, 15, and 16. The increasing of the graph shows the growth of the oxide layer. Meanwhile, the decreasing graph indicated the oxide layer spallation. All the specimens with different ultrasonic treatment and different temperature oxidation represent the growth of the oxide layer. The specimen without spallation at 900 °C is the FeCrAl ultrasonic pre-treatment with SiC for 10 minutes only. At 1000 °C, FeCrAl pre-treatment with SiC 10 minutes,  $\text{Al}_2\text{O}_3$  10 minutes, and  $\text{Al}_2\text{O}_3$  30 minutes show no spallation. For the oxidation at 1100 °C, the FeCrAl pre-treatment with SiC 10 minutes and  $\text{Al}_2\text{O}_3$  20 minutes also shows no spallation.

Both types of FeCrAl ultrasonic pre-treatment graphs were analyzed to obtain the estimation of parabolic rate constant as listed in Table 6 for FeCrAl ultrasonic pre-treatments with SiC or  $\text{Al}_2\text{O}_3$  oxidized at 900 °C, Table 7 for 1000 °C and Table 8 for 1100 °C. The lowest parabolic rate constants of FeCrAl ultrasonic pre-treatment with SiC are shown by its sonication time, as follows: after oxidation at 900 °C for 10 minutes, 1000 °C for 10 minutes, and 1100 °C for 30 minutes. Meanwhile, the lowest parabolic rate constant of FeCrAl ultrasonic pre-treatments with  $\text{Al}_2\text{O}_3$  are oxidized at 900 °C for 30 minutes, 1000 °C for 30 minutes, and 1100 °C for 30 minutes.

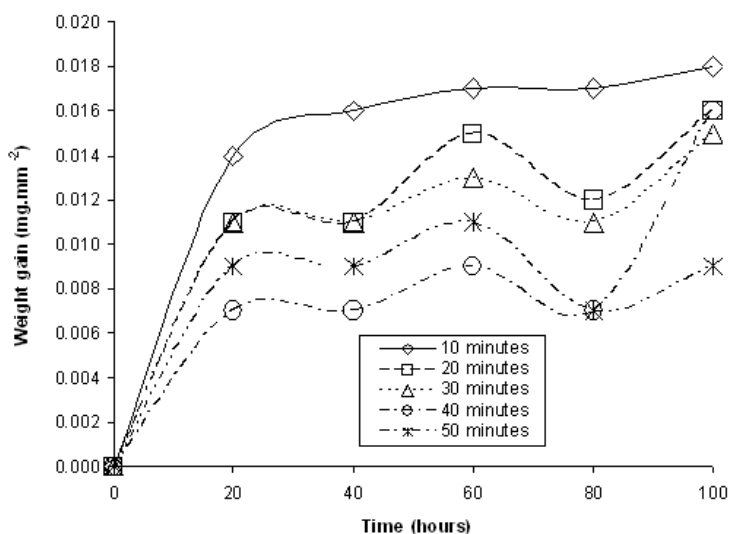


Fig. 11. Influence of various pre-treatment times on weight gain of FeCrAl treated using ultrasonic with SiC prior to nickel electroplating during oxidation at 900 °C using cyclic approach

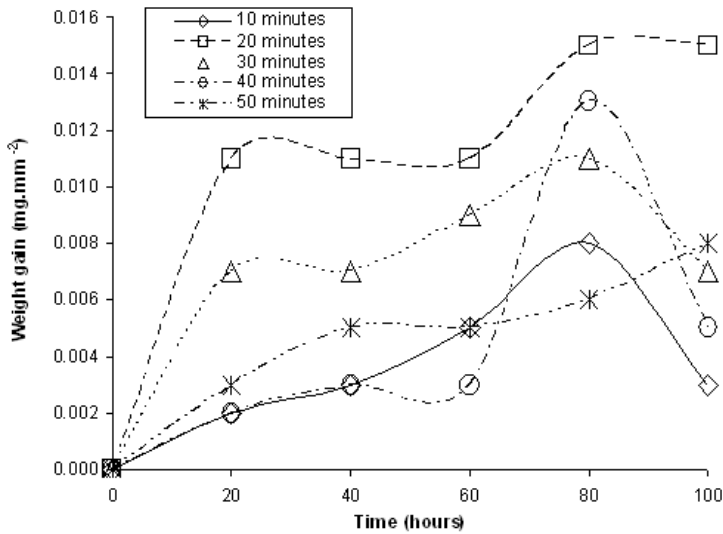


Fig. 12. Influence of various pre-treatment times on weight gain of FeCrAl treated using ultrasonic with SiC prior to nickel electroplating during oxidation at  $1000^\circ\text{C}$  using cyclic approach

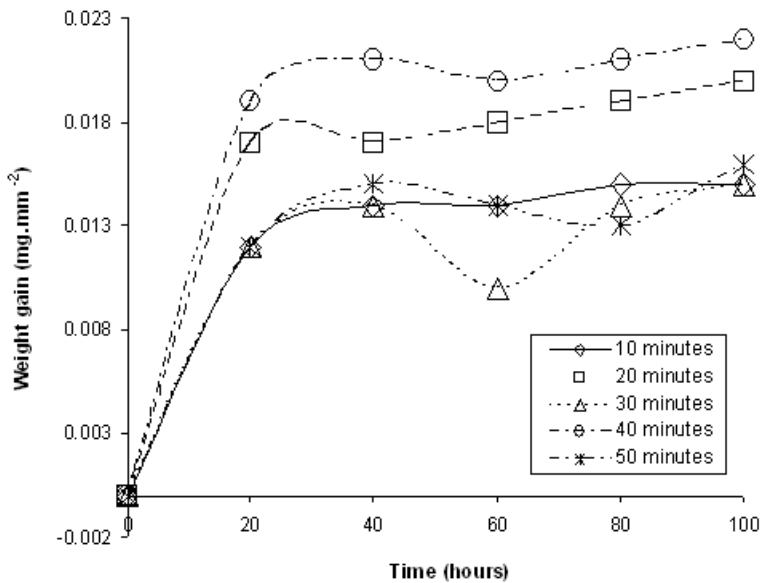


Fig. 13. Influence of various pre-treatment times on weight gain of FeCrAl treated using ultrasonic with SiC prior to nickel electroplating during oxidation at  $1100^\circ\text{C}$  using cyclic approach



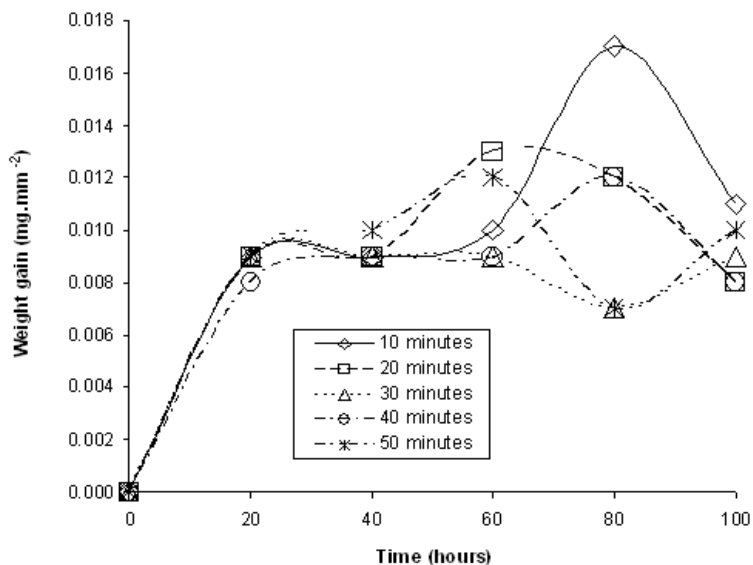


Fig. 14. Influence of various pre-treatment times on weight gain of FeCrAl treated using ultrasonic with Al<sub>2</sub>O<sub>3</sub> prior to nickel electroplating during oxidation at 900 °C using cyclic approach.

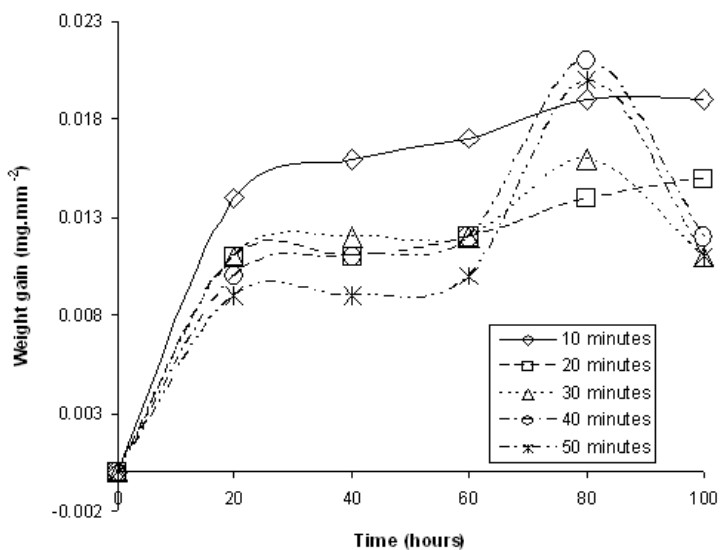


Fig. 15. Influence of various pre-treatment times on weight gain of FeCrAl treated using ultrasonic with Al<sub>2</sub>O<sub>3</sub> prior to nickel electroplating during oxidation at 1000 °C using cyclic approach

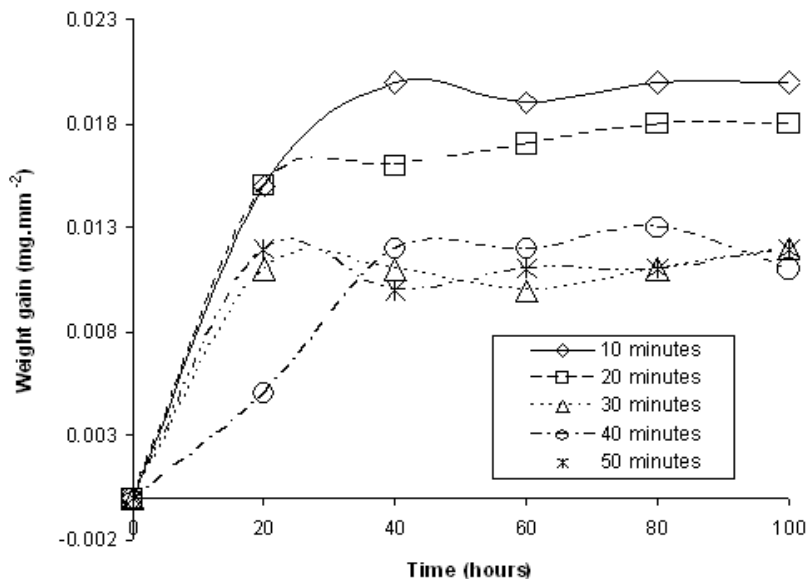


Fig. 16. Influence of various pre-treatment times on weight gain of FeCrAl treated using ultrasonic with  $\text{Al}_2\text{O}_3$  prior to nickel electroplating during oxidation at  $1100\text{ }^\circ\text{C}$  using cyclic approach

Specimens	Sonication Time (minutes)	Parabolic Rate Constant $k_p \times 10^{-4} \text{ mg}^2\text{mm}^{-4}\text{h}^{-1}$
FeCrAl ultrasonic pre-treatment with SiC	10	2.32
	20	1.87
	30	1.74
	40	1.42
	50	1.21
FeCrAl ultrasonic pre-treatment with $\text{Al}_2\text{O}_3$	10	1.64
	20	1.40
	30	1.15
	40	1.28
	50	1.30

Table 6. Parabolic rate constant ( $k_p$ ) of FeCrAl treated using ultrasonic and electroplating methods and oxidized at  $900\text{ }^\circ\text{C}$

The table of parabolic rate constant of oxidation test at  $900\text{ }^\circ\text{C}$  showed that the lowest parabolic rate constant obtained from FeCrAl ultrasonic treatment with SiC for 50 minutes at  $1.21 \times 10^{-4} \text{ mg}^2\text{mm}^{-4}\text{h}^{-1}$ , and FeCrAl ultrasonic treatment with  $\text{Al}_2\text{O}_3$  for 30 minutes at  $1.15 \times 10^{-4} \text{ mg}^2\text{mm}^{-4}\text{h}^{-1}$ . The lower parabolic rate constant indicated the longer time to failure of the FeCrAl substrate (Klower, et al., 1998). It can be seen from the table of parabolic rate constant at  $900\text{ }^\circ\text{C}$ , that longer pre-treatment process with SiC influenced to lower parabolic constant of FeCrAl, but it was not fully applied in pre-treatment with  $\text{Al}_2\text{O}_3$ .

Specimens	Sonication Time (minutes)	Parabolic Rate Constant $k_p \times 10^{-4} \text{ mg}^2\text{mm}^{-4}\text{h}^{-1}$
FeCrAl ultrasonic pre-treatment with SiC	10	0.64
	20	1.83
	30	1.15
	40	0.85
	50	0.84
FeCrAl ultrasonic pre-treatment with Al <sub>2</sub> O <sub>3</sub>	10	2.44
	20	1.82
	30	1.73
	40	1.92
	50	1.75

Table 7. Parabolic rate constant ( $k_p$ ) of FeCrAl treated using ultrasonic and electroplating methods and oxidized at 1000 °C

Specimens	Sonication Time (minutes)	Parabolic Rate Constant $k_p \times 10^{-4} \text{ mg}^2\text{mm}^{-4}\text{h}^{-1}$
FeCrAl ultrasonic pre-treatment with SiC	10	1.97
	20	2.55
	30	1.83
	40	2.86
	50	1.96
FeCrAl ultrasonic pre-treatment with Al <sub>2</sub> O <sub>3</sub>	10	2.65
	20	2.36
	30	1.52
	40	1.56
	50	1.54

Table 8. Parabolic rate constant ( $k_p$ ) of FeCrAl treated using ultrasonic and electroplating methods and oxidized at 1100 °C

In FeCrAl after oxidation at 1000 °C, the lowest parabolic rate constant for pre-treatment with SiC obtained for 10 minutes and with Al<sub>2</sub>O<sub>3</sub> for 30 minutes. There was no linear relation between ultrasonic pre-treatment and parabolic rate constant oxidation test at 1000 °C. However, there are some results by using ultrasonic with SiC powders obtained lower parabolic rate constant, under  $1 \times 10^{-4} \text{ mg}^2\text{mm}^{-4}\text{h}^{-1}$ , than pre-treatment with Al<sub>2</sub>O<sub>3</sub> after oxidation at 1000 °C. The very low parabolic rate constant of FeCrAl pre-treatment ultrasonic with SiC occurred for 10 minutes in  $0.64 \times 10^{-4} \text{ mg}^2\text{mm}^{-4}\text{h}^{-1}$ , for 50 minutes in  $0.84 \times 10^{-4} \text{ mg}^2\text{mm}^{-4}\text{h}^{-1}$ , and for 40 minutes in  $0.85 \times 10^{-4} \text{ mg}^2\text{mm}^{-4}\text{h}^{-1}$ . Meanwhile, ultrasonic pre-treatment with Al<sub>2</sub>O<sub>3</sub> resulted in  $1 \times 10^{-4} \text{ mg}^2\text{mm}^{-4}\text{h}^{-1}$  after oxidation at 1000 °C for 100 hours.

According to the parabolic rate constant table of specimens after oxidation at 1100 °C all the parabolic rates constant are higher than  $1 \times 10^{-4} \text{ mg}^2\text{mm}^{-4}\text{h}^{-1}$ . From the parabolic rate constant results, it can be estimated that both kind FeCrAl ultrasonic pre-treatment with SiC or Al<sub>2</sub>O<sub>3</sub> when oxidized at 1100 °C will be fail faster than those oxidized at 900 and 1100 °C. It is generally known that higher temperature caused faster material failures.

### 3.3.2 Cross section analysis of $\text{Al}_2\text{O}_3$ and NiO layers

Figure 17 presents cross section scanning electron micrograph with EDX line analysis of the NiO catalyst samples prepared on FeCrAl substrate through ultrasonic with SiC for 50 minutes (Figure 17.a),  $\text{Al}_2\text{O}_3$  30 minutes (Figure 17.b), then combined with nickel electroplating, and oxidation process at 900 °C. The EDX line analysis shows that nickel layer disappeared and fully converted to nickel oxide. Until the end of the oxidation exposure, the nickel oxide still existed.

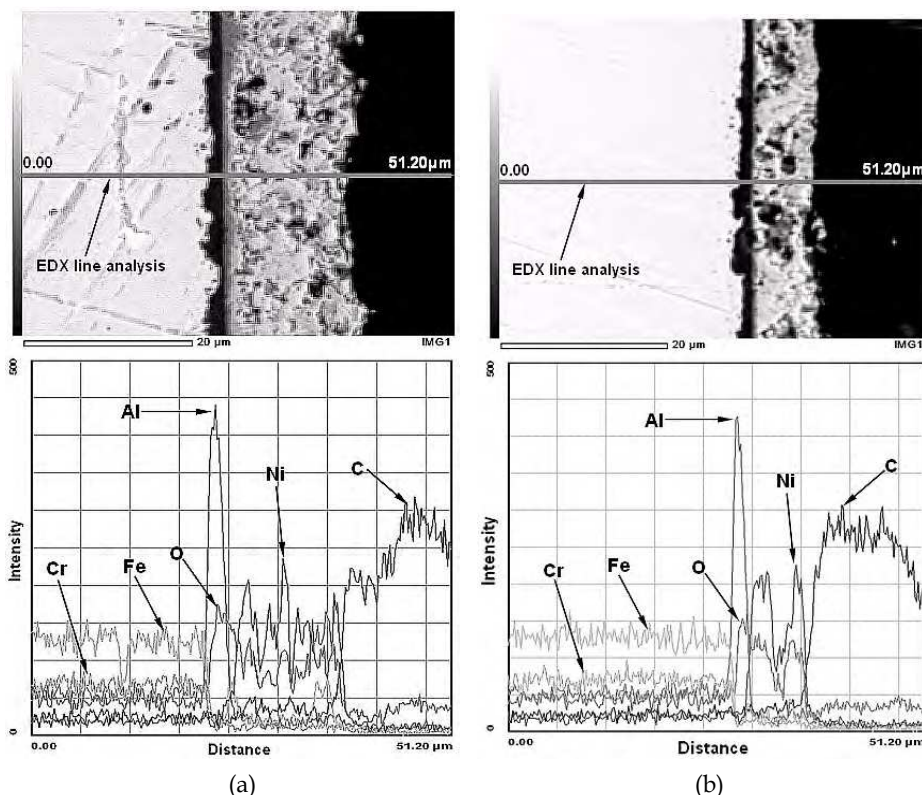


Fig. 17. Cross section scanning electron micrograph showing EDX line analysis (from left to right) of FeCrAl ultrasonic with (a) SiC for 50 minutes, (b)  $\text{Al}_2\text{O}_3$  for 30 minutes prior to nickel electroplating and oxidized at 900 °C with its chemical's intensity graph

Figure 18 shows cross section scanning electron micrograph with EDX line analysis of the NiO catalyst samples which developed on FeCrAl substrate through ultrasonic with SiC for 10 minutes (Figure 18.a),  $\text{Al}_2\text{O}_3$  for 30 minutes (Figure 18.b), then combined with nickel electroplating, and oxidation process at 1000 °C. According to the EDX line analysis, it is clear that both types of the FeCrAl whether treated by ultrasonic with SiC or  $\text{Al}_2\text{O}_3$  then electroplated with nickel showed the phase change of nickel to nickel oxide and existing of nickel oxide during oxidation exposure for 100 hours.

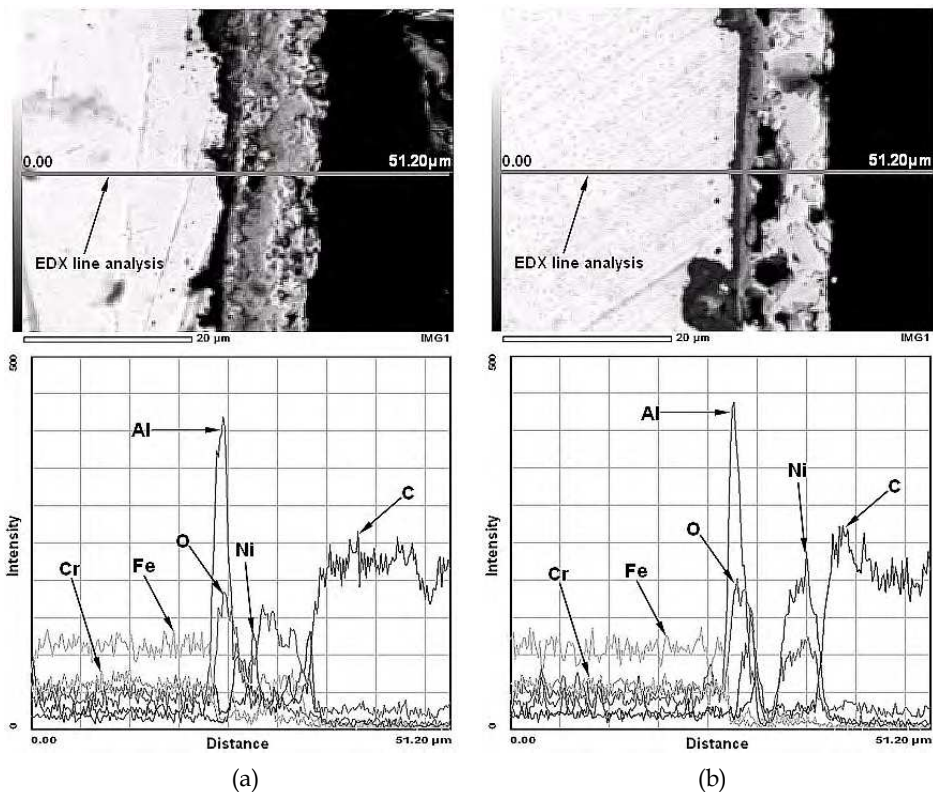


Fig. 18. Cross section scanning electron micrograph showing EDX line analysis (from left to the right) of FeCrAl ultrasonic with (a) SiC for 10 minutes, (b) Al<sub>2</sub>O<sub>3</sub> for 30 minutes prior to nickel electroplating and oxidized at 1000 °C with its chemical's intensity graph

Figure 19 shows cross section scanning electron micrograph with EDX line analysis of the NiO catalyst samples which prepared on FeCrAl substrate through ultrasonic with SiC for 30 minutes (Figure 19.a), Al<sub>2</sub>O<sub>3</sub> 30 minutes (Figure 19.b), then combined with nickel electroplating, and oxidation process at 1100 °C. The nickel phase layer completely changed to be nickel oxide phase. It showed that the nickel oxide still existed during the oxidation exposure.

From the cross section SEM/EDX (Fig. 17, 18 and 19), it is clearly that the nickel layer disappeared due to full conversion to nickel oxide during 100 hour oxidation processes. The large amount of the nickel oxide present in the outer oxide layer. The nickel oxide still existed although it seems several spallations after the oxidation process. The spallation occurred due to the influence of 100 hours oxidation. Besides NiO and Al<sub>2</sub>O<sub>3</sub> layers, according to chemical's graph there are several oxide layers or scale, which occurred as Cr<sub>2</sub>O<sub>3</sub> and Fe<sub>2</sub>O<sub>3</sub>. The Al<sub>2</sub>O<sub>3</sub> layer also occurred in stable condition as shown in the cross section image. Both specimens showed the evolution of nickel layer on the FeCrAl surface substrate, where it was fully converted to nickel oxide after oxidation exposure for 100 hours.

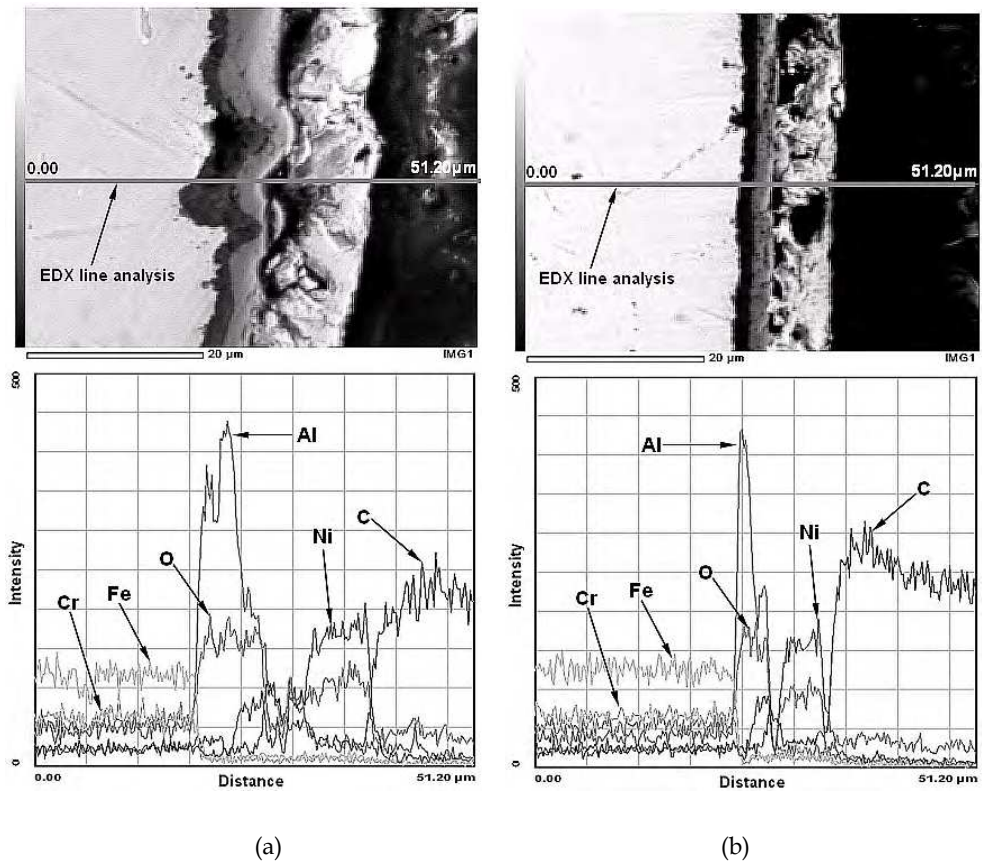


Fig. 19. Cross section scanning electron micrograph showing EDX line analysis (from left to the right) of FeCrAl ultrasonic with (a) SiC for 30 minutes, (b)  $\text{Al}_2\text{O}_3$  for 30 minutes prior to nickel electroplating, and oxidized at 1100 °C with its chemical's intensity graph

#### 4. Conclusion

A systematic study was conducted to evaluate the new method of developing NiO through oxidation in combination between nickel electroplating and ultrasonic technique. The NiO was obtained when treated at short term of oxidation for 6 hours at 900 °C and fully developed for 100 hours after oxidation at 900, 1000 and 1100 °C. The NiO catalyst successfully developed from nickel plating, which obtained on the surface of FeCrAl substrate through the electroplating combined with the ultrasonic process and oxidation process. For future work, the chemical properties of nickel oxide catalyst prepared on

FeCrAl substrate through the ultrasonic technique combined with the electroplating and oxidation process will be further investigated.

## 5. Acknowledgements

The authors would like to thank the Ministry of Higher Education Malaysia and Universiti Tun Hussein Onn Malaysia (UTHM) through the funding support of Fundamental Research Grant Scheme (FRGS), Vot no. 0265 and 0361. The authors would also like to thank Dr. W.J. Quadackers from Juelich Research Centre and the ThyssenKrupp VDM GmbH for providing the material.

## 6. References

- Amano, T.; Takezawa, Y.; Shiino, A. & Shishido, T. (2008). Surface Morphology of Scale on FeCrAl (Pd, Pt, Y) alloys. *Journal of Alloys and Compounds*, Vol. 452, No. 1, pp. 16-22
- American Society for Testing and Materilas [ASTM]. (1996). Standard Practice for Simple Static Oxidation Testing. America: G 54-84.
- Badini, C. & Laurella, F. (2001). Oxidation of FeCrAl Alloy: Influence of Temperature and Atmosphere on Scale Growth Rate and Mechanism. *Surface and Coating Technology*, Vol. 135, No. 2-3, pp. 291-298
- Benson, M.; Bennett, C.R.; Harry, J.E.; Patel, M.K. & M. Cross. (2000). The Recovery Mechanism of Platinum Group Metals from Catalytic Converters in Spent Automotive Exhaust Systems. *Resources, Conservation and Recycling*, Vol. 31, No. 1, pp. 1-7
- Birks, N.; Meier, G.H. & F.S. Pettit. (2006). *Introduction to The High Temperature Oxidation of Metals*, 2<sup>nd</sup> ed, Cambridge University Press, ISBN 978-0-511-16089-9, New York, USA
- Checmanowski, J.G. & Szczygiel, B. (2008). High Temperature Oxidation Resistance of FeCrAl Alloys Covered with Ceramic SiO<sub>2</sub>-Al<sub>2</sub>O<sub>3</sub> Coatings Deposited by Sol-gel Method. *Corrosion Science*, Vol. 50, No. 12, pp. 3581-3589
- Chiba, A.; Gotou, T.; Kobayashi, K. & Wu, W. (2000). Influence of sonication of nickel plating in a nickel sulfamate bath. *Metal Finishing*, Vol. 98, No. 9, pp. 66-69
- Corni, I.; Ryan, M.P. & Boccaccini, A.R. (2008). Electrophoretic deposition: From traditional ceramics to nanotechnology. *Journal of the European Ceramic Society*, Vol. 28, No. 7, pp. 1353-1367
- Cueff, R.; Buscail, H.; Caudron, E.; Riffard, F.; Issartel, C. & El Meski, S. (2004). Effect of Reactive Element Oxide Coating on the High Temperature Oxidation Behaviour of FeCrAl Alloys. *Applied Surface Science*, Vol. 229, No. 1-4, pp. 233-241
- Czyrska-Filemonowicz, A.; Szot, K.; Wasilkowska, A.; Gil, A. & Quadackers, W.J. (1999). Microscopy (AFM, TEM, SEM) Studies of Oxide Scale Formation on FeCrAl Based ODS Alloys. *Solid State Ionics*, Vol. 117, No. 1-2, pp. 13-27

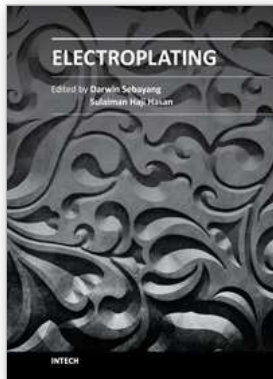
- Eleta, A.; Navarro, P.; Costa, L. & Montes, M. (2009). Deposition of zeolitic coatings onto FeCrAlloy microchannels: Washcoating vs. in situ growing. *Microporous and Mesoporous Materials*, Vol. 123, No. 1-3, pp. 113-122
- Fukuda, K.; Takao, K.; Hoshi, T. & Furukumi, O. (2002). Improved High Temperature Oxidation Resistance of REM Added Fe-20%Cr-5%Al Alloy by Pre-Annealing Treatment. In: *Materials Aspects in Automotive Catalytic Converters*, Hans Bode (Ed.), 59-82, Wiley-VCH Verlag GmbH, ISBN 3-527-30491-6, Weinheim, Germany
- Heck, R. M.; Farrauto, R. J. & Gulati, S. T. (2002). *Catalytic Air Pollution Control Commercial Technology 3<sup>rd</sup> ed*, John Wiley & Sons, ISBN 978 -0-470-27503-0, New Jersey
- Henke, L.; Nagy, N. & Krull, U.J. (2002). An AFM determination of the effects on surface roughness caused by cleaning of fused silica and glass substrates in the process. *Biosensors and Bioelectronics*, Vol. 17, pp. 547-555
- Huang, Y. & Bar-Ilan, A. (2003). *Method for washcoating a catalytic material onto a monolithic structure*. U. S. Patent 6759358
- Jia, L.; Shen, M. & Wang, J. (2007). Preparation and characterization of dip-coated  $\gamma$ -alumina based ceramic materials on FeCrAl foils. *Surface & Coatings Technology*, Vol. 201, No. 16-17, pp. 7159-7165
- Klöwer, J.; Kolb-Telieps, A.; Bode, H.; Brede, M.; Lange, J.; Brück, R. & Wieres, L. (1998). Development of high-temperature corrosion resistant FeCrAl alloys for automotive catalytic converters. *Materials Week Congress for Innovative Materials, Processes, and Applications*, Munich, Germany, 12-15.10.1998
- Kolaczowski, S. (2006). Treatment of Volatile Organic Carbon (VOC) Emissions from Stationary Sources: Catalytic Oxidation of The Gaseous Phase. In: *Structured Catalysts and Reactors 2<sup>nd</sup> ed*, A. Cybulski. & J. A. Moulijn, (Eds.), 147-169, Taylor & Francis Group, ISBN 0-8247-2343-0, Boca Raton, FL
- Koltsakis, G.C. & Stamatelos, A.M. (1997). Catalytic Automotive Exhaust After Treatment. *Progress in Energy and Combustion Science*, Vol. 23, No. 1, pp. 1-39
- Liu, G.; Rozniatowski, K. & Kurzydowski, K.J. (2001). Quantitative Characteristics of FeCrAl Films Deposited by Arc and High-velocity Arc Spraying. *Materials Characterization*, Vol. 46, No. 2-3, pp. 99-104
- Lylykangas, R. & Tuomola, H. (2002). A New Type of Metallic Substrate. In: *Materials Aspects in Automotive Catalytic Converters*, Hans Bode (Ed.), 152-170, Wiley-VCH Verlag GmbH, ISBN 3-527-30491-6, Weinheim, Germany
- Mies, M.J.M.; Rebrov, E.V.; Jansen, J.C.; Croon, M.H.J.M. & Schouten, J.C. (2007). Hydrothermal synthesis of a continuous zeolite Beta layer by optimization of time, temperature and heating rate of the precursor mixture. *Microporous and Mesoporous Materials*, Vol. 106, No. 1-3, pp. 95-106
- Nicholls, J. R. & Quadackers, W. J. (2002). Materials Issues Relevant to the Development of Future Metal Foil Automotive Catalytic Converters. In: *Materials Aspects in Automotive Catalytic Converters*, Hans Bode (Ed.), 31-48, Wiley-VCH Verlag GmbH, ISBN 3-527-30491-6, Weinheim, Germany



- Pilone, D. (2009). Ferritic Stainless Steels for High Temperature Applications in Oxidizing Environments. *Recent Patents on Materials Science*, Vol. 2, No. 1, pp. 27-31, ISSN 1874-4648
- Rose, I. & Whittington, C. (2002). *Nickel Plating Handbook*. OMG Group, Finland
- Sivaiah, M.V.; Petit, S.; Beaufort, M.F.; Eyidi, D.; Barrault, J.; Batiot-Dupeyrat, C. & Valange, S. (2010). Nickel based catalysts derived from hydrothermally synthesized 1:1 and 2:1 phyllosilicate as precursors for carbon dioxide reforming of methane. *Microporous and Mesoporous Materials*, Vol. 140, No. 1-3, pp. 69-80
- Smallman, R.E. & Bishop, R.J. (1999). *Modern Physical Metallurgy and Materials Engineering Science, Process, Applications 6<sup>th</sup> ed.* Butterworth-Heinemann Elsevier, ISBN 0-7506-4564-4, Oxford.
- Specchia, A.; Civera, A. & Saracco, G. (2004). In situ combustion synthesis of perovskite catalysts for efficient and clean methane premixed metal burner. *Chemical Engineering Science*, Vol. 59, No. 22-23, pp. 5091-5098
- Sun, H.; Quan, X.; Chen, S.; Zhao, H. & Zhao, Y. (2007). Preparation of well-adhered g-Al<sub>2</sub>O<sub>3</sub> washcoat on metallic wire mesh monoliths by electrophoretic deposition. *Applied Surface Scienc*, 253, pp. 3303-3310
- Suslick K.S.; Didenko, Y.; Fang, M.; Hyeon, T.; Kolbeck, K.J.; Mc Namara III, W.B.; Mdleleni, M.M. & Wong, M. (1999). Acoustic cavitation and its chemical consequences. *Philosophical Transactions: Mathematical, Physical and Engineering Sciences*, Vol. 357, pp. 335-353
- Taniguchi, S., Andoh, A., & Shibata, T. (2002). Improvement in The Oxidation Resistance of Al-deposited Fe-Cr-Al Foil by Pre-oxidation. In: *Materials Aspects in Automotive Catalytic Converters*, Hans Bode (Ed.), 83-105, Wiley-VCH Verlag GmbH, ISBN 3-527-30491-6, Weinheim, Germany
- Twigg, M. V. & Webster, D. E. (2006). Metal and Coated Metal Catalysts. In: *Structured Catalysts and Reactors 2<sup>nd</sup> ed.*, A. Cybulski. & J. A. Moulijn, (Eds.), 71-108, Taylor & Francis Group, ISBN 0-8247-2343-0, Boca Raton, FL
- Wei, Q.; Chen, Z.X.; Nie, Z.R.; Hao, Y.L.; Zou, J.X. & Wang, Z.H. (2005). Mesoporous activated alumina layers deposited on FeCrAl metallic substrates by an in situ hydrothermal method. *Journal of Alloys and Compounds*, Vol. 396, No. 1-2, pp. 283-287
- Wu, X.; Weng, D.; Zhao, S. & Chen, W. (2007). Influence of an aluminized intermediate layer on the adhesion of a g-Al<sub>2</sub>O<sub>3</sub> washcoat on FeCrAl. *Surface & Coatings Technology*, Vol. 190, No. 2-3, pp. 434- 439
- Yanqing, Z.; Jieming, X.; Cuiqing, L.; Xin, X. & Guohua, L. (2010). Influence of preparation method on performance of a metal supported perovskite catalyst for combustion of methane. *Journal of Rare Earths*, Vol. 28, No. 1, pp. 54-58
- Zamaro, JM.; Ulla, M.A. & Miro, E.E. (2008). ZSM5 growth on a FeCrAl steel support. Coating characteristics upon the catalytic behavior in the NO<sub>x</sub> SCR. *Microporous and Mesoporous Materials*, Vol. 115, No. 1-2, pp. 113-122

---

Zhao, S.; Zhang, J.; Weng, D. & Wu, X. (2003). A method to form well-adhered  $\gamma$ -Al<sub>2</sub>O<sub>3</sub> layers on FeCrAl metallic supports. *Surface and Coating Technology*, Vol. 167, No. 1, pp. 97-105



## **Electroplating**

Edited by Prof. Darwin Sebayang

ISBN 978-953-51-0471-1

Hard cover, 166 pages

**Publisher** InTech

**Published online** 11, April, 2012

**Published in print edition** April, 2012

This book emphasizes on new applications of electroplating with consideration for environmental aspect and experimental design. Written by experienced expert from various countries, the authors come from academia and electroplating industrial players. Here, a very detailed explanation to the new application of the electroplating is followed by a solution of the environmental issue caused by the electroplating process and concluded by experimental design for optimization of electro deposition processes.

Coverage included:

- Preparation NiO catalyst on FeCrAl Substrate Using Various Technique at Higher Oxidation Process
- Electrochemical properties of carbon- supported metal nanoparticle prepared by electroplating methods
- Fabrication of InGaN-Based Vertical Light Emitting Diodes Using Electroplating
- Integration Of Electrografted Layers for the Metallization of Deep Through Silicon Vias
- Biomass adsorbent for removal of toxic metal ions from electroplating industry wastewater
- Resistant fungal biodiversity of electroplating effluent and their metal tolerance index
- Experimental design and response surface analysis as available tools for statistical modeling and optimization of electrodeposition processes

### **How to reference**

In order to correctly reference this scholarly work, feel free to copy and paste the following:

Darwin Sebayang, Yanuandri Putrasari, Sulaiman Hasan, Mohd Ashraf Othman and Pudji Untoro (2012). Preparation of NiO Catalyst on FeCrAl Substrate Using Various Techniques at Higher Oxidation Process, Electroplating, Prof. Darwin Sebayang (Ed.), ISBN: 978-953-51-0471-1, InTech, Available from: <http://www.intechopen.com/books/electroplating/preparation-of-nio-catalyst-on-fecral-substrate-using-various-techniques-at-higher-oxidation-process>

**INTECH**  
open science | open minds

### **InTech Europe**

University Campus STeP Ri  
Slavka Krautzeka 83/A  
51000 Rijeka, Croatia  
Phone: +385 (51) 770 447

### **InTech China**

Unit 405, Office Block, Hotel Equatorial Shanghai  
No.65, Yan An Road (West), Shanghai, 200040, China  
中国上海市延安西路65号上海国际贵都大饭店办公楼405单元  
Phone: +86-21-62489820

Fax: +385 (51) 686 166  
www.intechopen.com

Fax: +86-21-62489821

© 2012 The Author(s). Licensee IntechOpen. This is an open access article distributed under the terms of the [Creative Commons Attribution 3.0 License](#), which permits unrestricted use, distribution, and reproduction in any medium, provided the original work is properly cited.